Evolution of supraorbital ossification in Charadriiformes

Author: Hughes, Austin L.

Source: The Auk, 132(3) : 685-696

Published By: American Ornithological Society

URL: https://doi.org/10.1642/AUK-14-274.1

The Auk
Ornithological Advances
AmericanOrnithology.org

Volume 132, 2015, pp. 685–696
DOI: 10.1642/AUK-14-274.1

RESEARCH ARTICLE

Evolution of supraorbital ossification in Charadriiformes

Austin L. Hughes

Department of Biological Sciences, University of South Carolina, Columbia, South Carolina, USA
austin@biol.sc.edu

Submitted November 28, 2014; Accepted March 25, 2015; Published June 10, 2015

ABSTRACT

Phylogenetic analysis of morphological data on 92 species in the order Charadriiformes showed that increased supraorbital ossification (SO) has evolved independently at least 4 times in this clade. Principal component analysis of size-corrected skeletal measures showed that an evolutionary increase in SO was associated with a body plan in which the cranium, humerus, and sternum were relatively large. A mass-corrected measure of the axial length of the eye was positively correlated with a mass-corrected measure of cranium length, both in the raw data and in phylogenetically independent contrasts. By revealing an association between the evolution of SO and increased relative size of the eye and flight-associated skeletal elements, these results support the hypothesis that an increased reliance on visually guided foraging in flight or diving has been a major selective factor favoring the evolution of increased SO in Charadriiformes.

Keywords: body plan, character reconstruction, shorebirds, supraorbital ossification

Évolution de l'ossification supraorbitaire chez les Charadriiformes

RÉSUMÉ

L'analyse des données morphologiques de 92 espèces de Charadriiformes, dans un cadre phylogénétique, a montré qu'une ossification supraorbitaire (OS) accrue a évolué indépendamment au moins quatre fois dans ce clade. Une analyse en composantes principales de mesures squelettiques corrigées pour la taille a montré qu'un accroissement évolutif de l'OS était associé à un schéma corporel dans lequel le crâne, l'humérus et le sternum étaient relativement gros. Une mesure corrigée pour la masse de la longueur axiale de l'œil était positivement corrélée avec une mesure corrigée pour la masse de la longueur du crâne, à la fois dans les données brutes et dans les contrastes phylogénétiquement indépendants. En révélant une association entre l'évolution de l'OS et une augmentation de la taille relative de l'œil et des éléments squelettiques associés au vol, ces résultats supportent l'hypothèse qu'une dépendance accrue à l'égard de la quête alimentaire guidée par la vue, en vol ou en plongée, a été un important facteur sélectif favorisant l'évolution d'une OS accrue chez les Charadriiformes.

Mots-clés: schéma corporel, reconstruction des caractères, limicoles, ossification supraorbitaire

INTRODUCTION

In a study of the visual field of 2 species in the order Charadriiformes, the Red Knot (*Calidris canutus*) and the European Golden-Plover (*Pluvialis apricaria*), Martin and Piersma (2009) associated aspects of cranial morphology with differences in feeding strategy between the 2 species. They reported a greater field of binocular vision in the Red Knot than in the European Golden-Plover, which they suggested represents an adaptation to visually guided probing with the bill in the Red Knot (Martin and Piersma 2009). By contrast, the European Golden-Plover has relatively large eyes, supported by a bone that Martin and Piersma (2009) named the "supraorbital aliform bone" (os supraorbitale aliforme). Martin and Piersma (2009) suggest that the large eyes of the European Golden-Plover represent, at least in part, an adaptation to nocturnal feeding.

The Charadriiformes form a large and ecologically diverse order of birds including 3 suborders (Charadrii, Lari, and Scolopaci), in which distinct lineages have adapted convergently to similar ecological niches (Colwell 2010). Supraorbital ossification (SO) broadly similar to that observed in the European Golden-Plover has been reported in other species in this order, particularly in suborder Lari (e.g., Strauch 1985). Indeed, although the homology of such structures has not been studied, some form of SO occurs in birds belonging to a number of orders (Livezey and Zusi 2006). Comparative analysis thus has the potential to shed light on the evolutionary origin of SO and its role as a component of a suite of morphological and behavioral adaptations.

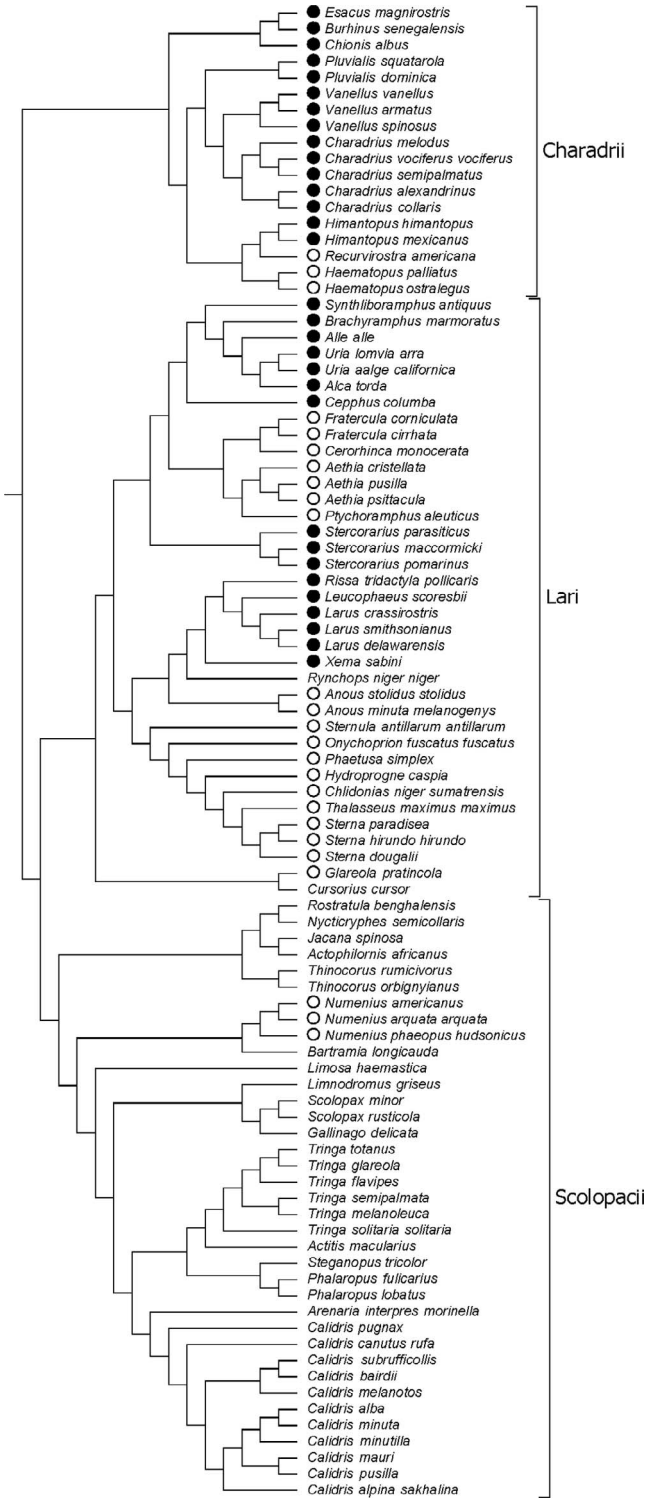

FIGURE 1. Phylogenetic relationships of the 92 charadriiform species used in this study, based on Jetz et al. (2012). Character state of supraorbital ossification is indicated as follows: open circle = partial; solid circle = full.

The tremendous diversity of body plans seen in birds reflects the numerous distinct ecological niches to which birds have adapted (Feduccia 1996). The relative measurements of major skeletal elements can yield simple quantitative indices of overall body plan, which can be used to test comparative hypotheses regarding ecological adaptations (Hughes 2013, 2014). Here, I survey the pattern of SO in 92 species in Charadriiformes, representing all 3 suborders. I then relate the patterns of SO with body plan, thereby shedding light on the ecological forces that may influence this trait.

METHODS

Specimens and Measurements

I examined skeletal specimens (from the Field Museum of Natural History, Chicago, Illinois, USA, and the U.S. National Museum of Natural History, Washington, D.C.) of 92 species in Charadriiformes (Supplemental Material Table S1 and Appendix Figure 7). The cranial morphology, including SO, was examined on at least 1 adult male and 1 adult female of each species and on other individuals if available. Taxonomy and nomenclature followed Clements et al. (2014). Subspecies designations were used when museum specimens were identified to subspecies, and all specimens used for a given species were derived from the same subspecies. The selection of species was based on the availability of at least 1 adult male skeleton and at least 1 adult female skeleton, with the goal of sampling as much of the diversity of Charadriiformes as possible. All 3 suborders (Charadrii, Lari, and Scolopaci) were represented by multiple species (Figure 1). Phylogenetic relationships (Figure 1) were assumed to follow Jetz et al. (2012). Many, but not all, clades in this tree were supported in the phylogeny of Thomas et al. (2004). One major exception is that Jetz et al. (2012), following Baker et al. (2007), placed Stercorariidae as a sister group to Alcidae. On the other hand, the comprehensive morphology-based phylogeny of Livezey and Zusi (2007) agreed with Thomas et al. (2004) regarding the placement of Stercorariidae. Because of this and other discrepancies, I conducted separate analyses assuming (1) the phylogeny of Figure 1 and (2) the phylogeny of Thomas et al. (2004; Appendix Figure 7).

The following 9 skeletal measurements (Baumel and Witmer 1993) were made by digital caliper on 1 adult male and 1 adult female of each species in the sample (Supplemental Material Table S1): (1) maxilla, measured from the dorsal junction of the maxilla with the cranium to the tip of the bill (rostrum maxillare); (2) cranium, measured from the nasofrontal hinge to the posterior end (prominentia cerebellaris) of the cranium; (3) sternum length (sternum L), measured from apex carinae to margo caudalis; (4) sternum width (sternum W), measured just anterior to the base of the trabeculae laterales; (5)

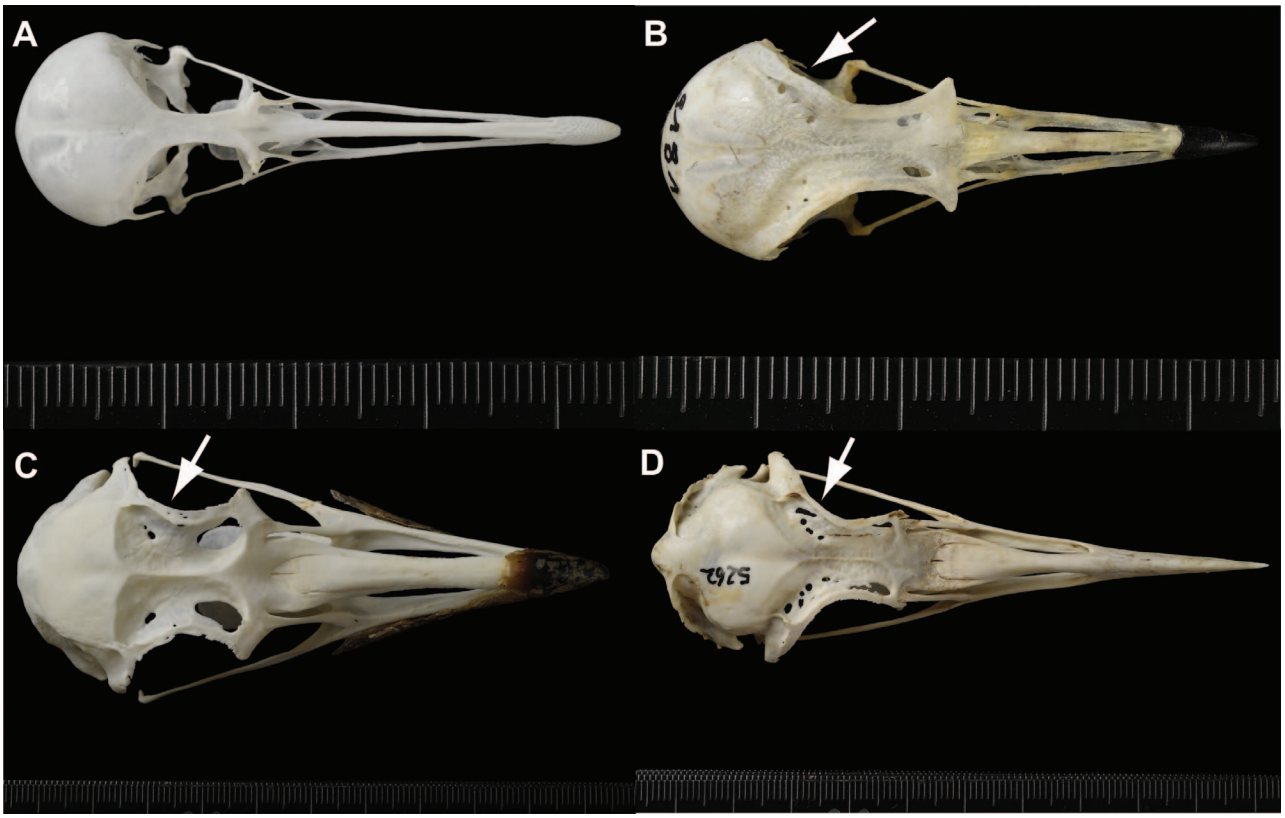

FIGURE 2. Crania of (**A**) Sanderling (*Calidris alba*), (**B**) Common Ringed Plover (*Charadrius hiaticula*), (**C**) Great Skua (*Stercorarius skua*), and (**D**) Common Murre (*Uria aalge*). Supraorbital ossification is indicated by arrows. Scale bars are in millimeters. Photo credit: G. Mayr

humerus, measured from the apex of caput humeri to the caudal edge between condylus ventralis and processus flexorius; (6) synsacrum length (synsacrum L), measured from the anterior edge of ala preacetabularis to the tip of the posterior projection of the ilium; (7) synsacrum width (synsacrum W), measured just posterior to foramen ilioischiadicum; (8) femur, measured from facies articularis antitrochanterica to sulcus intercondylaris; and (9) tibiotarsus, measured from the proximal point of facies gastrocnemialis to incisura intercondylaris. To obtain an average value for each species that incorporates at least some of the within-species variation, the male and female measurements were averaged to yield a single mean value of each measurement for the species.

Mean body-mass values (g) for each species were obtained from Dunning (2008). When mean values for males and females were given separately, the mean of those 2 means was used. For 1 species in the sample (*Nycticryphes semicollaris*), data were not available in Dunning (2008); for this species, I used the midpoint of the body-mass range provided by del Hoyo et al. (1996). Axial lengths (AL) of the eyes of 48 of the species in the sample were obtained from Howland et al. (2004) and Møller and Erritzøe (2010).

Supraorbital Ossification

I defined SO operationally as the possession a bony ridge or ridges extending over the rear and/or top of the orbit, showing evidence of fusion to the frontal bone and having a maximum width equal to at least one-fifth the width of the skull (i.e. the distance between the outer rims of the frontal bones on either side of the skull) measured at the apex of the orbit. Species were placed into 3 categories: (1) SO was scored as absent (A) in species in which the rim of the frontal bone formed a smooth curve from processus postorbitalis to the most dorsolateral edge of os lacrimale (Figure 2A). (2) SO was scored as full (F) in species in which SO covered >50% of the rim of the orbit between processus postorbitalis to the most dorsolateral edge of os lacrimale (Figure 2B–2D). This character is illustrated for Alcidae in Strauch (1985: fig. 3B), for the European Golden-Plover in Martin and Piersma (2009), and for the Mew Gull (*Larus canus*) in De Pietri et al. (2011: fig. 3D). (3) SO was scored as partial (P) in species in which SO covered <50% of the rim of the orbit, at the rear (Figure 3). This character is illustrated for Alcidae in Strauch (1985: fig. 3A), for the Brown Noddy (*Anous stolidus*) in De Pietri et al. (2011: fig. 3B), and for the Arctic Tern (*Sterna paradisaea*) in De Pietri et al. (2011: fig. 3C).

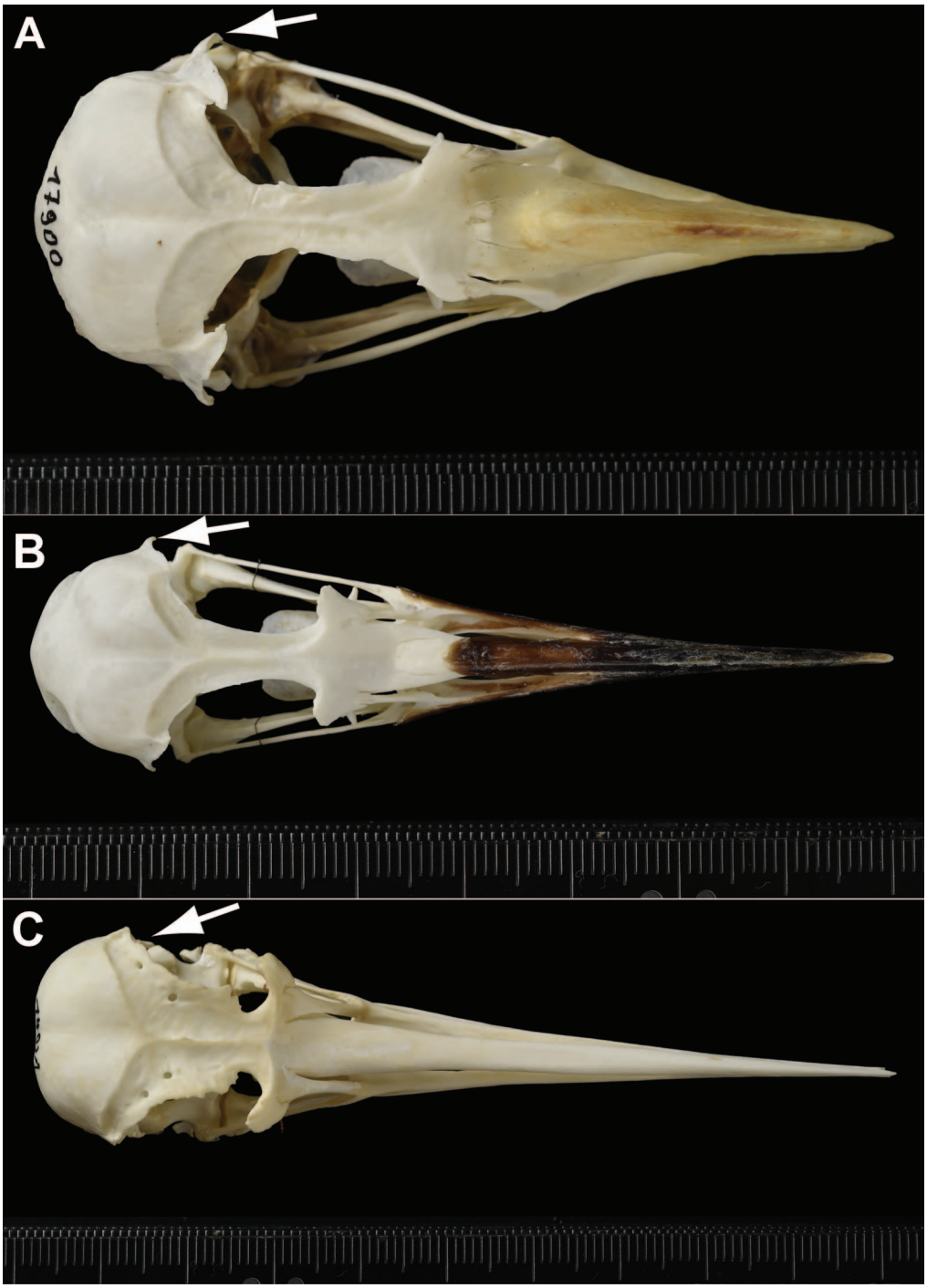

FIGURE 3. Crania of (**A**) Atlantic Puffin (*Fratercula arctica*), (**B**) Sooty Tern (*Onychoprion fuscatus*), and (**C**) Eurasian Oystercatcher (*Haematopus ostralegus*). Supraorbital ossification is indicated by arrows. Scale bars are in millimeters. Photo credit: G. Mayr

Size-corrected Measures

Measurements were corrected for body size in 2 ways: by Mosimann transformations and by mass-corrected measures.

Mosimann transformations. Size-corrected transformations (Mosimann 1970) were computed from the natural logarithm of the mean value (for male and female) of the 9 skeletal measurements. Where x_i are the individual measurements, let $z_i = \ln[x_i/G(x)]$, where $G(x)$ is the geometric mean of the 9 measurements within each species (Mosimann 1970). The resulting values (z_i) are referred to here as "Z-variables." Principal component

analysis of the *Z*-variables was used to provide size-independent indices of body shape for each species (Darroch and Mosimann 1985, Jungers et al. 1995, Hughes 2013, 2014). Jungers et al. (1995) reviewed various size-corrected measures of body shape used in morphometrics and advocated the approach employed here.

Mass-corrected measures. The transformation proposed by Lleonart et al. (2000) was used to obtain measures corrected for body mass. For any measure Y having an allometric relationship with another measure X, the transformation $Y_i^* = Y_i[X_0/X_i]^b$, where X_0 is the mean of the X_i values and b is the allometric exponent (Lleonart et al. 2000). The latter transformation was applied both to AL and to the 9 skeletal measures. In the case of the 9 skeletal measures, the resulting transformed values were highly positively correlated with the *Z*-variables (not shown). Therefore, only analyses based on the *Z*-variables are reported here for the 9 skeletal measures. However, Lleonart et al.'s (2000) transformation was used for AL and was used in addition to the *Z*-variables for comparisons between AL and skeletal measures.

Statistical Analyses

Because the assumption of statistical independence made by most conventional statistical tests is not warranted in the case of data derived from phylogenetically related species (Harvey and Pagel 1991), statistical analyses involving the *Z*-variables and principal components derived from them were conducted in 2 ways, by randomization tests and by explicitly phylogenetic analyses, neither of which required the assumption of independence.

Randomization tests. Each randomization test involved creating 10,000 pseudo-datasets by sampling (with replacement) from the data. For comparison of 2 means, the absolute difference between the mean values in the observed data was compared with the distribution of absolute differences in the pseudo-datasets. For tests of correlation coefficients, the absolute value of the correlation coefficient in the observed data was compared with the distribution of the absolute values of correlation coefficients observed in the pseudo-datasets.

Explicitly phylogenetic analyses. Ancestral character reconstruction for SO was conducted by maximum parsimony in Mesquite version 2.75 (Maddison and Maddison 2011), assuming the phylogenetic tree of Figure 1. For purposes of parsimony reconstruction, 2 species in the order Gruiformes, the Gray-throated Rail (*Canirallus oculeus*) and the Common Crane (*Grus grus*), were used as an outgroup.

Phylogenetically independent PDAP contrasts (Garland et al. 1992) were estimated in Mesquite, using arbitrary branch lengths. For each variable used in PDAP contrasts, the correlation between the absolute values of contrasts and their standard errors was used to test for adequacy of standardization (Garland et al. 1992); no significant correlations were found.

All reported *P* values are 2-tailed. Means are reported ± SE. Statistical analyses were conducted in Minitab version 15 (see Acknowledgments).

RESULTS

Supraorbital Morphology

Most members of the suborder Scolopaci, as well as the Cream-colored Courser (*Cursorius cursor*) in the suborder Lari, showed SO character state A (Figure 1). The Pectoral Sandpiper (*Calidris melanotos*) provides an example of this type of cranial morphology (Figure 2A), very similar to that reported for the Red Knot by Martin and Piersma (2009). Martin and Piersma (2009) suggested an association between the lack of SO and forward-directed eyes; but the woodcocks (genus *Scolopax*), in spite of having eyes backward-directed rather than forward-directed, resembled most other Scolopaci in lacking SO.

A cranial morphology (corresponding to the F state of SO) similar to that described for the European Golden-Plover by Martin and Piersma (2009), including an alate supraorbital bone, was seen in all species in the family Charadriidae examined here, as illustrated by the cranium of the Piping Plover (*Charadrius melodus*; Figure 2B). The F state was also seen in several lineages of suborder Lari; examples include the South Polar Skua (*Stercorarius maccormicki*; Figure 2C) and the Common Murre (*Uria aalge*; Figure 2D).

In addition to the F character state of SO, certain members of all 3 suborders showed the P state. In puffins (genera *Cerorhinca* and *Fratercula*), the ossification took the form of an alate bone at the rear of the orbit (Figure 3A). The terns (Lari: Sternidae) showed a somewhat similar postorbital ossification, although with a less sharply defined alate form (Figure 3B). In the oystercatchers (Charadrii: Haematopodidae), there was also postorbital ossification, although without any sign of an alate form (Figure 3C). A similar pattern was also seen in the Collared Pratincole (*Glareola pratincola*), although the one other species in the family Glareolidae included in the present dataset, the Cream-colored Courser, showed no SO.

Evolution of Supraorbital Ossification

Using Gruiformes as an outgroup to determine the ancestral state of SO in Charadriiformes, A was inferred to be the ancestral state of the order (Figure 4). Although several nodes were ambiguous, there was evidence that increased SO has evolved independently in each of the 3 suborders. In Scolopaci, there has been an A→P transition in the branch leading to the most recent common ancestor (MRCA) of *Numenius* (Figure 4). Although the character

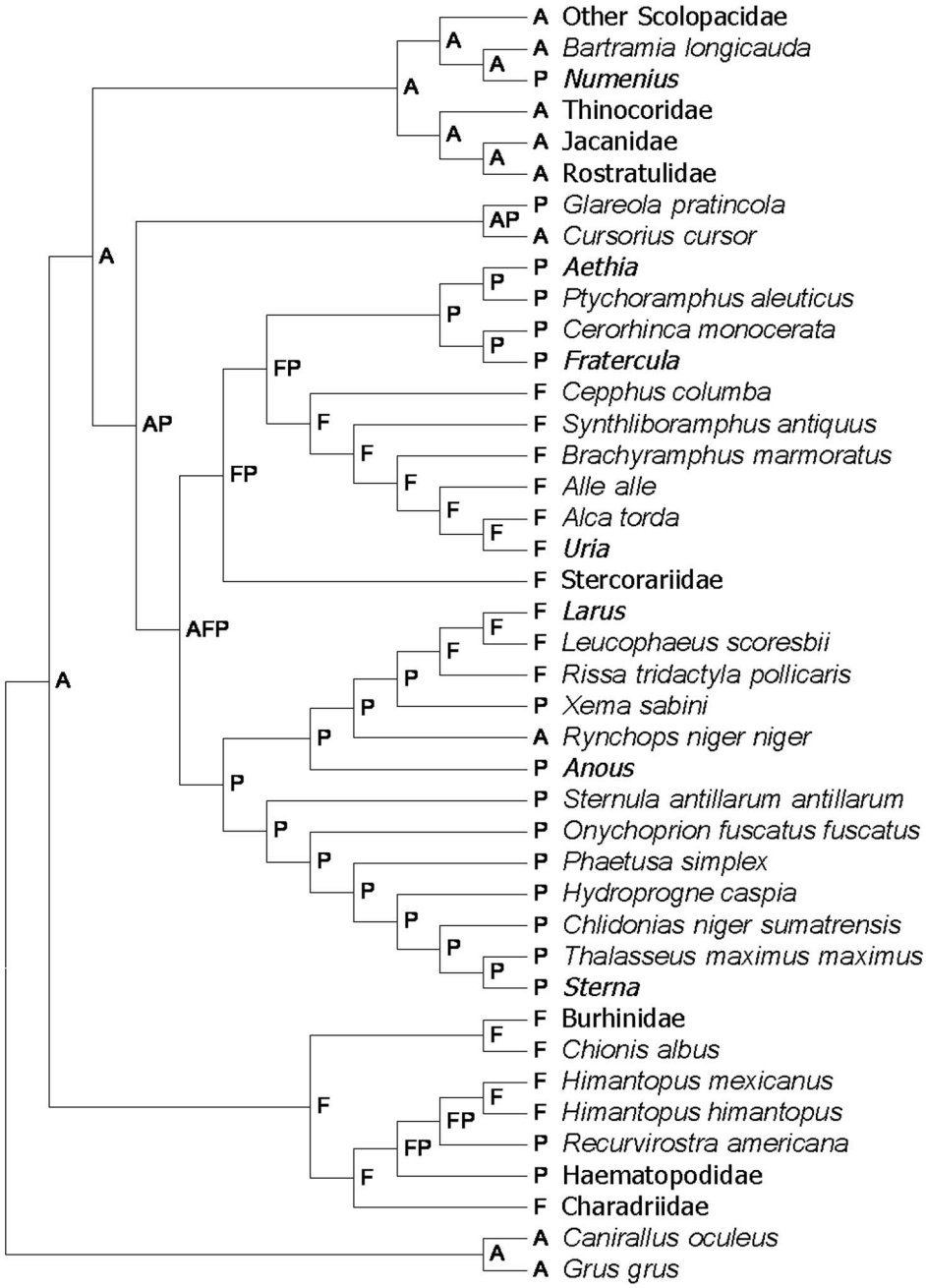

FIGURE 4. Parsimony reconstruction of the evolution of supraorbital ossification (SO) character state (A = absent, P = partial, or F = full) in Charadriiformes. Clades uniform with respect to SO are condensed. Plus sign on a branch indicates an increase in SO. When a node was ambiguous for 2 character states, both are shown (e.g., "AP").

state of the MRCA of Lari could not be determined, the results supported the hypothesis that the common ancestor of Scolopaci and Lari had character state A (Figure 4); this, in turn, implied that SO evolved independently in these 2 suborders. Assuming the phylogeny of Figure 1, there was at least 1 transition within Lari to greater SO: namely, a P→F transition in the branch leading to the MRCA of *Rissa*, *Leucophaeus*, and *Larus* (Figure 4). Finally, because the analysis supported the hypothesis that A was the character state of the common ancestor of the 3 charadriiform suborders (Figure 4), the results supported a further independent evolution of SO in Charadrii.

Assuming the phylogeny of Appendix Figure 7, independent evolution of SO in each of the 3 suborders was again supported (Appendix Figure 8). In addition, on the

TABLE 1. Variable loadings on the first 2 principal components (PC1 and PC2) derived from transformed skeletal measurements of 92 species in the order Charadriiformes.

Skeletal measure	PC1	PC2
Maxilla	0.420	0.209
Cranium	−0.262	0.355
Sternum length	−0.429	−0.269
Sternum width	−0.482	0.007
Humerus	−0.287	0.334
Synsacrum length	−0.273	−0.346
Synsacrum width	0.218	0.197
Femur	0.072	−0.607
Tibiotarsus	0.360	−0.323
Percent variance	31.7%	21.2%

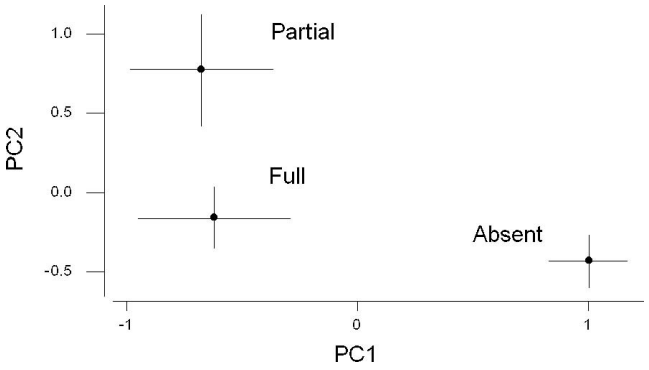

FIGURE 5. Mean (with SE bars) of PC1 and PC2 scores in the 3 clusters of charadriiform species based on supraorbital ossification character state: absent, partial, or full.

basis of the latter phylogeny, 2 additional transitions to increased SO were reconstructed within Lari: (1) an A→F or P→F transition in the branch leading to the MRCA of Stercoraridae; and (2) a P→F transition in the branch leading to the MRCA of the genera *Alca*, *Alle*, *Brachyramphus*, *Cepphus*, *Synthliboramphus*, and *Uria* (Appendix Figure 8).

Indices of Body Form

Together, the first 2 principal components (PC1 and PC2) extracted from the correlation matrix of the *Z*-variables accounted for 52.9% of the variance (Table 1). PC1 contrasted the relative length of the maxilla and tibiotarsus and the relative width of the synsacrum with the other measurements. Species scoring high on PC1 were thus species with relatively long bills and legs. The species receiving the 4 highest PC1 scores were the Black-necked Stilt (*Himantopus mexicanus*), the Black-winged Stilt (*H. himantopus*), the American Avocet (*Recurvirostra americana*), and the Short-billed Dowitcher (*Limnodromus griseus*) (Supplemental Material Table S1). The species receiving the 4 lowest PC1 scores were all in the Alcidae: the Ancient Murrelet (*Synthliboramphus antiquus*), the Crested Auklet (*Aethia cristatella*), the Thick-billed Murre (*Uria lomvia arra*), and the Razorbill (*Alca torda*) (Supplemental Material Table S1).

PC2 primarily contrasted the relative lengths of cranium and humerus with the relative lengths of tibiotarsus, femur, and synsacrum (Table 1). Thus, species with high PC2 scores had relatively large head and humerus but relatively short legs. The 4 highest PC2 scores were found among the Sternidae: in the Black Tern (*Chlidonias niger sumatrensis*), the Common Tern (*Sterna hirundo hirundo*), the Black Noddy (*Anous minutus melanogenys*), and the Least Tern (*Sternula antillarum antillarum*) (Supplemental Material Table S1). The 4 lowest PC2 scores were found in a much more taxonomically diverse group, with representatives of all 3 charadriiform suborders: the Gray-breasted Seedsnipe (*Thinocorus orbignyianus*), the Crested Auklet (*Aethia cristatella*), the Snowy Sheathbill (*Chionis albus*), and the African Jacana (*Actophilornis africana*) (Supplemental Material Table S1).

Species Categorized by Character State

The 92 species were placed in 3 groups based on SO: A ($n = 36$ species), P ($n = 26$), and F ($n = 30$). The mean PC1 score in the A group (1.006 ± 0.172) was significantly greater than that in the P group (–0.677 ± 0.315; randomization test, $P < 0.001$) and significantly greater than that in the F group (–0.620 ± 0.335; randomization test, $P < 0.001$) (Figure 5). On the other hand, the mean PC1 score did not differ significantly between the P group and the F group (randomization test; Figure 5). The mean PC2 score in the A group (–0.431 ± 0.169) was significantly less than that in the P group (0.778 ± 0.354; randomization test, $P < 0.001$) but did not differ significantly from that in the F group (–0.157 ± 0.195; randomization test) (Figure 5). The mean PC2 score also differed significantly between the P group and the F group (randomization test, $P < 0.011$; Figure 5). Thus, the A group was characterized by generally high PC1 scores and low PC2 scores (Figure 5). The P and F groups showed similarly low PC1 scores but were distinguished by the generally high PC2 scores in the P group (Figure 5).

The basis for these differences among the 3 groups was further examined by comparing means of the *Z*-variables between groups (Table 2). The A group was distinguished from the P and F groups by having significantly smaller relative length of the cranium, significantly smaller relative length of the humerus, significantly smaller length of the synsacrum, and significantly greater relative length of the femur (Table 2). The A group also showed a significantly greater relative length of the tibiotarsus than the P group and a significantly greater relative length of the maxilla than the F group (Table 2). The P and F groups were distinguished by relatively greater maxilla length in the former and relatively greater tibiotarsus length in the

TABLE 2. Size-corrected measures (means ± SE) of the relative size of skeletal elements (*Z*-variables) in charadriiform species categorized on the basis of supraorbital ossification (A = absent, P = partial, and F = full; NS = nonsignificant).

	Supraorbital ossification			*P* (randomization test)		
Skeletal measure	A ($n = 36$)	P ($n = 26$)	F ($n = 30$)	A vs. P	A. vs F	P vs. F
Maxilla	0.262 ± 0.052	0.156 ± 0.066	−0.051 ± 0.034	NS	<0.001	<0.012
Cranium	−0.252 ± 0.019	−0.137 ± 0.043	−0.173 ± 0.017	<0.003	<0.040	NS
Sternum length	0.334 ± 0.015	0.414 ± 0.043	0.432 ± 0.045	NS	NS	NS
Sternum width	−0.625 ± 0.022	−0.574 ± 0.022	−0.580 ± 0.023	NS	NS	NS
Humerus	0.260 ± 0.015	0.431 ± 0.019	0.439 ± 0.027	<0.001	<0.001	NS
Synsacrum length	0.060 ± 0.011	0.118 ± 0.012	0.133 ± 0.016	NS	<0.020	NS
Synsacrum width	−0.528 ± 0.019	−0.578 ± 0.030	−0.596 ± 0.040	NS	NS	NS
Femur	−0.130 ± 0.014	−0.227 ± 0.019	−0.180 ± 0.015	<0.001	<0.025	NS
Tibiotarsus	0.579 ± 0.025	0.399 ± 0.030	0.581 ± 0.037	<0.001	NS	<0.001

former. Thus, the A group was distinguished from the P and F groups by a relatively small cranium and humerus, whereas the P group was characterized by a relatively longer cranium and shorter legs than the A and F groups.

Eye Size

In order to examine the relationship between cranium size and eye size, I tested for correlation between the mass-corrected AL of the eye and the mass-corrected length of the cranium for 48 species for which AL data were available. There was a highly significant positive correlation between the 2 variables (randomization test, $r = 0.666$, $P < 0.001$; Figure 6). Similarly, there was a highly significant positive correlation between mass-corrected AL and the *Z*-variable for cranium length (randomization test, $r = 0.496$, $P < 0.001$). Assuming the phylogeny of Figure 1, there was a positive correlation between phylogenetically independent PDAP contrasts in mass-corrected AL and those in mass-corrected cranium length ($r = 0.439$, $P = 0.002$). Likewise, there was a positive correlation between PDAP contrasts in mass-corrected AL and those in the *Z*-variable for cranium ($r = 0.368$, $P = 0.042$).

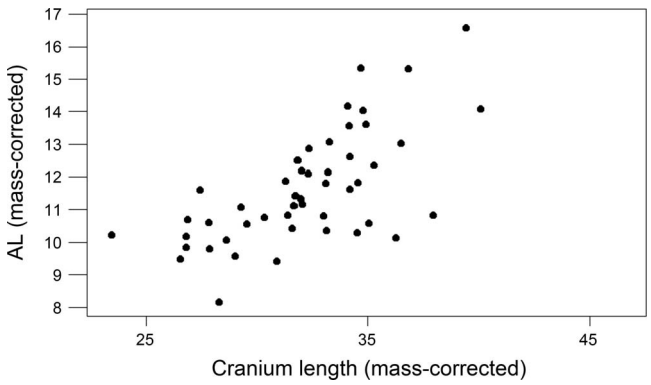

FIGURE 6. Plot of the mass-corrected axial length (AL) of the eye versus the mass-corrected length of the cranium for 48 charadriiform species (randomization test, $r = 0.666$, $P < 0.001$).

Assuming the phylogeny of Appendix Figure 7, there was a significant positive correlation between PDAP contrasts in mass-corrected AL and those in mass-corrected cranium length ($r = 0.425$, $P = 0.004$). Likewise, there was a positive correlation between PDAP contrasts in mass-corrected AL and those in the *Z*-variable for cranium length ($r = 0.552$, $P < 0.001$). Thus, the differences between the 2 phylogenies did not affect the positive relationship between AL and relative cranium size.

The 48 species with AL data included 28 from the A group, 4 from the P group, and 16 from the F group. Mean mass-corrected AL was significantly greater in the F species (12.9 ± 0.4 mm) than in the A species (11.0 ± 0.2; randomization test, $P < 0.001$). Mean mass-corrected AL was likewise significantly greater in the F species than in the P species (11.0 ± 1.6 mm; randomization test, $P < 0.04$).

DISCUSSION

A phylogenetic approach indicated that SO has evolved independently at least 4 or 5 times in the Charadriiformes. Martin and Piersma (2009) hypothesized that SO in the European Golden-Plover is associated with large, laterally directed eyes, which in turn are associated with nocturnal foraging. The present analysis revealed an association between SO and a relatively long cranium, as well as a relatively long humerus and large sternum, as reflected in low PC1 scores (Table 1 and Figure 5). The association of SO with a relatively long cranium is consistent with an association between SO and the possession of large, laterally directed eyes. Moreover, the present results also showed a strong positive correlation between mass-adjusted AL of the eye and mass-adjusted cranium length, thus supporting an association between SO and relatively large eyes. A positive correlation between head size and eye size is generally observed in birds, but this correlation mainly reflects the effect of overall body size (Brooke et al. 1999, Burton 2008). The present finding of a positive

correlation between eye AL and cranium length in Charadriiformes, even after controlling for the effect of body size, represents the first such report in any avian order. This correlation was seen in phylogenetically independent contrasts as well as in the original data, indicating that the coevolution of cranium length and eye size has been a persistent tendency throughout the evolutionary history of the order.

Species lacking SO tended to have relatively long bills and legs, as indicated by high PC1 scores (Table 1 and Figure 5). This result is consistent with the association proposed by Martin and Piersma (2009) between the absence of SO and a pattern of foraging behavior involving wading in shallow water, in which the bill is guided either tactilely or by partially forward-directed eyes. In addition, the present analyses provided evidence that charadriiform species lacking SO have relatively small eyes in relation to body size.

The frequent evolution of increased SO in the order Charadriiformes implies that selection favoring this trait has acted repeatedly on diverse lineages within the order. Although nocturnal foraging may be one selective factor favoring the maintenance of relatively large eyes and, thus, of SO in certain charadriiform species (Thomas et al. 2006, Hall and Ross 2007), the present results argue against it as a general explanation for the evolution of SO in the order as a whole. Increased SO has evolved independently in groups not known for nocturnal foraging, including the family-level taxa Haematopodidae, Chionidae, Stercorariidae, and Laridae and the subfamily Alcinae (Thomas et al. 2006).

Several studies have compared the relative size of the eyes or of brain regions important for vision (the optic lobes or optic tecta) across various sets of avian taxa, including some evidence regarding Charadriiformes. The factors found to be associated with relatively large visual structures appear to be related mainly to an important role of flight in foraging. Species that rely on predation guided by vision in flight have relatively large eyes (Brooke et al. 1999) and relatively large optic tecta (Iwaniuk and Hurd 2005). Consistent with this finding, physiological studies support the importance of large, laterally directed eyes in the detection of movement by visually guided predators, including terns (Land 1999, Tucker 2000). Conversely, the evolution of flightlessness in the Alcidae has been associated with reduction in the relative size of the optic lobes (Smith and Clarke 2012).

The limited data available from Charadriiformes show larger relative optic tecta in 1 tern species (Sternidae) and in 2 plover species (Charadriidae) than in 2 sandpiper species (Iwaniuk and Hurd 2005). These findings are consistent with Martin and Piersma's (2009) comparison of visual fields and feeding strategies in the European Golden-Plover and the Red Knot. The present analyses revealed an association in Charadriiformes between relatively large eyes and a relatively large sternum and long humerus. In Charadiiformes, a relatively large sternum and long humerus are likely to have been associated with increased reliance on flight in foraging—and, in Alcidae, also with wing-propelled diving (Smith and Clarke 2014). The present results show that a relatively large cranium, relatively long humerus, and relatively large sternum are also associated with SO. This suggests, in turn, that an increased reliance on visually guided foraging in flight or diving has been a major selective factor that has favored the repeated evolution of SO in Charadriiformes.

Although some degree of SO is typical of marine species in suborder Lari, the present results do not suggest a strong relationship between the presence of SO and reliance on salt secretion by the nasal glands (Schmidt-Nielsen 1960). The size of the nasal gland in relation to body mass shows substantial within-species variability in Charadriiformes, depending on the salinity of the environment (Gutiérrez et al. 2012). Both plover species possessing SO and sandpiper species lacking SO show an essentially identical pattern of substantial increase in nasal-gland mass when foraging in marine coastal habitats (Gutiérrez et al. 2012). The nasal-gland mass in coastally foraging plovers and sandpipers was measured at ~0.1% of body mass (Gutiérrez et al. 2012), comparable to values reported for marine members of Alcidae and Laridae (Fänge et al. 1958, Staaland 1967, Peaker and Linzell 1975). Among the 21 charadriiform species whose nasal glands were examined by Staaland (1967), the highest ratio of nasal gland to body mass (0.12%) was in the Red Knot, which lacks SO; this ratio is substantially higher than those reported for guillemots (genera *Cepphus* and *Uria*), the Razorbill (*Alca torda*), and the Dovekie (*Alle alle*), all marine taxa scored as having the F state of SO in the present study (Figure 1). Conversely, it is of interest that SO is only partial in some marine taxa in this order (e.g., terns and some alcids; Figure 1), covering only the rear of the orbit and thus little of the nasal glands. Nonetheless, it remains a viable hypothesis that the size and shape of SO may reflect adaptation to use of the nasal glands in salt excretion by certain marine taxa in this order.

The combined effect of multiple selective pressures acting on a suite of individual phenotypic traits can result in a coevolutionary process giving rise to a distinctive multidimensional phenotype (Pigliucci 2003). As a consequence, the adaptive significance of any individual trait is likely to be best understood in the context of other traits with which it is associated to form such a phenotypic complex. The results of the present study illustrate the usefulness of measures of the relative size of avian skeletal elements for deriving simple indices of body plan (such as principal components) that can reduce complex, multidimensional patterns to a linear scale (Hughes 2013, 2014).

Examining the associations between such indices and other morphological, physiological, ecological, and life history traits can, in turn, be used to help formulate and test hypotheses regarding the adaptive significance of complex adaptive phenotypes. Furthermore, the present study illustrates the power of a comparative approach, in contrast to studies focused on only a few species, for testing hypotheses regarding the adaptive significance of complex phenotypic patterns.

ACKNOWLEDGMENTS

I am grateful to the staffs of the Field Museum of Natural History, especially B. Marks, and the U.S. National Museum of Natural History, especially B. Schmidt, for access to specimens. I am grateful to G. Mayr for the use of his photographs and for numerous comments that improved the manuscript. Minitab software is available online (http://www.minitab.com).

LITERATURE CITED

Baker, A. J., S. L. Pereira, and T. A. Paton (2007). Phylogenetic relationships and divergence times of Charadriiformes genera: Multigene evidence for the Cretaceous origin of at least 14 clades of shorebirds. Biology Letters 3:205–209.

Baumel, J. J., and L. M. Witmer (1993). Osteologia. In Handbook of Avian Anatomy: Nomina Anatomica Avium, second edition (J. J. Baumel, A. S. King, J. E. Breazile, H. E. Evans, and J. C. Vanden Berge, Editors), Publications of the Nuttall Ornithological Club 23, pp. 45–132.

Brooke, M. de L., S. Hanley, and S. B. Laughlin (1999). The scaling of eye size with body mass in birds. Proceedings of the Royal Society of London, Series B 266:405–412.

Burton, R. F. (2008). The scaling of eye size in adult birds: Relationship to brain, head and body sizes. Vision Research 48:2345–2351.

Clements, J. F., T. S. Schulenberg, M. J. Iliff, D. Roberson, T. A. Fredericks, B. L. Sullivan, and C. L. Wood (2014). The eBird/Clements Checklist of Birds of the World, version 6.9. http://www.birds.cornell.edu/clementschecklist/download/

Colwell, M. A. (2010). Shorebird Ecology, Conservation, and Management. University of California Press, Berkeley, CA, USA.

Darroch, J. N., and J. E. Mosimann (1985). Canonical and principal components of shape. Biometrika 72:241–252.

De Pietri, V. L., L. Costeur, M. Güntert, and G. Mayr (2011). A revision of the Lari (Aves, Charadriiformes) from the early Miocene of Saint-Gérand-le-Puy (Allier, France). Journal of Vertebrate Paleontology 31:812–828.

del Hoyo, J., A. Elliott, and J. Sargatal (Editors) (1996). Handbook of the Birds of the World, vol. 3. Lynx Edicions, Barcelona, Spain.

Dunning, J. B., Jr. (2008). CRC Handbook of Avian Body Masses, second edition. CRC Press, Boca Raton, FL, USA.

Fänge, R., K. Schmidt-Nielsen, and H. Osaki (1958). The salt gland of the Herring Gull. Biological Bulletin 115:162–171.

Feduccia, A. (1996). The Origin and Evolution of Birds. Yale University Press, New Haven, CT, USA.

Garland, T., Jr., P. H. Harvey, and A. R. Ives (1992). Procedures for the analysis of comparative data using phylogenetically independent contrasts. Systematic Biology 41:18–32.

Gutiérrez, J. S., M. W. Dietz, J. A. Masero, R. E. Gill, Jr., A. Dekinga, P. F. Battley, J. M. Sánchez-Guzmán, and T. Piersma (2012). Functional ecology of saltglands in shorebirds: Flexible responses to variable environmental conditions. Functional Ecology 26:236–244.

Hall, M. I., and C. F. Ross (2007). Eye shape and activity pattern in birds. Journal of Zoology 271:437–444.

Harvey, P. H., and M. D. Pagel (1991). The Comparative Method in Evolutionary Biology. Oxford University Press, Oxford, UK.

Howland, H. C., S. Merola, and J. R. Basarab (2004). The allometry and scaling of the size of vertebrate eyes. Vision Research 44:2043–2065.

Hughes, A. L. (2013). Indices of anseriform body shape based on the relative size of major skeletal elements and their relationship to reproductive effort. Ibis 155:835–846.

Hughes, A. L. (2014). Evolution of bill size in relation to body size in toucans and hornbills (Aves: Piciformes and Bucerotiformes). Zoologia 31:256–263.

Iwaniuk, A. N., and P. L. Hurd (2005). The evolution of cerebrotypes in birds. Brain, Behavior and Evolution 65:215–230.

Jetz, W., G. H. Thomas, J. B. Joy, K. Hartmann, and A. O. Mooers (2012). The global diversity of birds in space and time. Nature 491:444–448.

Jungers, W. L., A. B. Falsetti, and C. E. Wall (1995). Shape, relative size, and size-adjustments in morphometrics. American Journal of Physical Anthropology 38 (Supplement S2):137–161.

Land, M. F. (1999). The roles of head movements in the search and capture strategy of a tern (Aves, Laridae). Journal of Comparative Physiology A 184: 265–272.

Livezey, B. C., and R. L. Zusi (2006). Higher-order phylogeny of modern birds (Theropoda, Aves: Neornithes) based on comparative anatomy: I.—Methods and characters. Bulletin of the Carnegie Museum of Natural History 37.

Livezey, B. C., and R. L. Zusi (2007). Higher-order phylogeny of modern birds (Theropoda, Aves: Neornithes) based on comparative anatomy. II. Analysis and discussion. Zoological Journal of the Linnean Society 149:1–95.

Lleonart, J., J. Salat, and G. J. Torres (2000). Removing allometric effects of body size in morphological analysis. Journal of Theoretical Biology 205:85–93.

Maddison, W. P., and D. R. Maddison (2011). Mesquite: A Modular System for Evolutionary Analysis, version 2.75. http://mesquiteproject.org

Martin, G. R., and T. Piersma (2009). Vision and touch in relation to foraging and predator detection: Insightful contrasts between a plover and a sandpiper. Proceedings of the Royal Society of London, Series B 276:437–445.

Møller, A. P., and J. Erritzøe (2010). Flight distance and eye size in birds. Ethology 116:458–465.

Mosimann, J. E. (1970). Size allometry: Size and shape variables with characterizations of the lognormal and generalized gamma distributions. Journal of the American Statistical Association 65:930–945.

Peaker, M., and J. L. Linzell (1975). Salt Glands in Birds and Reptiles. Cambridge University Press, Cambridge, UK.

Pigliucci, M. (2003). Phenotypic integration: Studying the ecology and evolution of complex phenotypes. Ecology Letters 6:265–272.
Schmidt-Nielsen, K. (1960). The salt-secreting gland of marine birds. Circulation 21:955–967.
Smith, N. A., and J. A. Clarke (2012). Endocranial anatomy of the Charadriiformes: Sensory system variation and the evolution of wing-propelled diving. PLOS One 7:e49584.
Smith, N. A., and J. A. Clarke (2014). Systematics and evolution of the Pan-Alcidae (Aves, Charadriiformes). Journal of Avian Biology 45:1–16.
Staaland, H. (1967). Anatomical and physiological adaptations of the nasal glands in Charadriiformes birds. Comparative Biochemistry and Physiology 23:933–944.
Strauch, J. G., Jr. (1985). The phylogeny of the Alcidae. The Auk 102:520–539.
Thomas, G. H., M. A. Wills, and T. Székely (2004). A supertree approach to shorebird phylogeny. BMC Evolutionary Biology 4: 28.
Thomas, R. J., T. Székely, R. F. Powell, and I. C. Cuthill (2006). Eye size, foraging methods and the timing of foraging in shorebirds. Functional Ecology 20:157–165.
Tucker, V. A. (2000). The deep fovea, sideways vision and spiral flight paths in raptors. Journal of Experimental Biology 203: 3745–3754.

SUPPLEMENTAL MATERIAL TABLE S1. Measurements of skeletal specimens of 92 species in the order Charadriiformes examined for this study (from the Field Museum of Natural History, Chicago, Illinois, USA, and the U.S. National Museum of Natural History, Washington, D.C.) Available at doi: 10.1642/AUK-14-274.1

APPENDIX

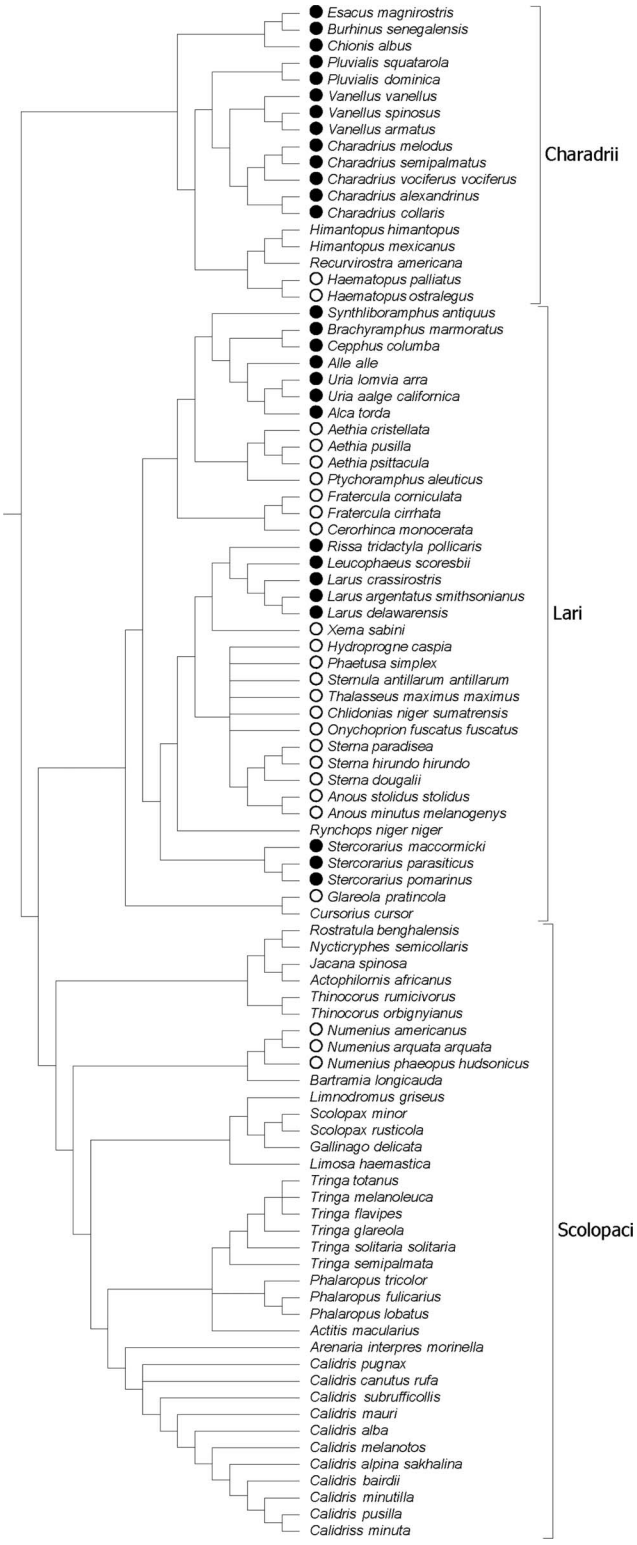

FIGURE 7. Alternative phylogeny of 92 species in the order Charadriiformes, based on Thomas et al. (2004).

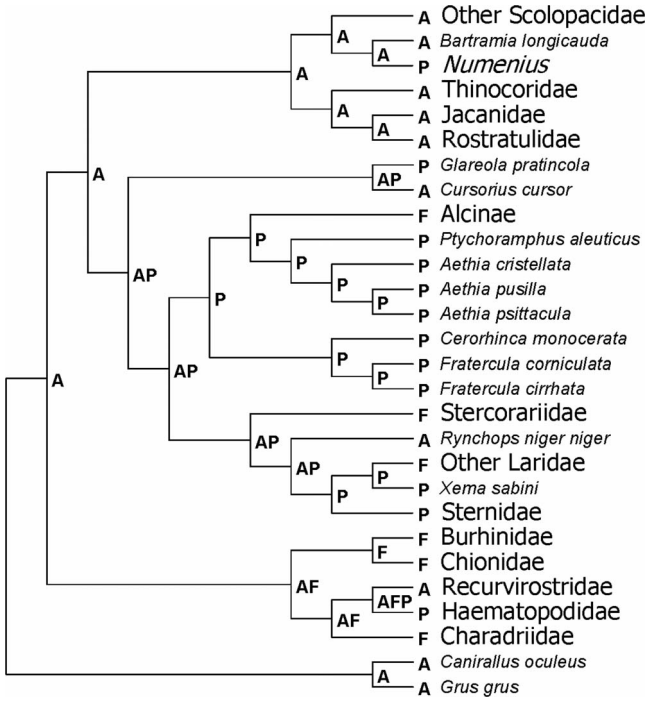

FIGURE 8. Reconstructed changes in supraorbital ossification in the order Charadriiformes, assuming the phylogeny of Appendix Figure 7.